

Gene expression responses *in vivo* by human telomerase reverse transcriptase (hTERT)-targeting *trans*-splicing ribozyme

Min-Sun Song¹, Jin-Sook Jeong², Kyung-Sook Cho³
and Seong-Wook Lee^{1,4}

¹Department of Molecular Biology
Institute of Nanosensor and Biotechnology
Dankook University
Yongin 448-701, Korea

²Department of Pathology
Medical Center for Cancer Molecular Therapy
Dong-A University College of Medicine
Busan 602-103, Korea

³Research Institute and Hospital
National Cancer Center
Goyang 411-764, Korea

⁴Corresponding author: Tel, 82-31-8005-3195;
Fax, 82-31-8005-4058; E-mail, SWL0208@dankook.ac.kr

Accepted 15 October 2007

Abbreviations: HCC, hepatocellular carcinoma; hTERT, human telomerase reverse transcriptase; PEPCK, phosphoenolpyruvate carboxykinase; PL, Ad-PEPCK-LacZ; PRL, Ad-PEPCK.Ribo-LacZ; TS, *trans*-splicing

Abstract

A *trans*-splicing ribozyme which can specifically re-program human telomerase reverse transcriptase (hTERT) RNA was previously suggested as a useful agent for tumor-targeted gene therapy. In this study, we evaluated *in vivo* function of the hTERT-targeting *trans*-splicing ribozymes by employing the molecular analysis of expression level of genes affected by the ribozyme delivery into peritoneal carcinomatosis mice model. To this effect, we constructed adenoviral vector encoding the specific ribozyme. Noticeably, more than four-fold reduction in the level of hTERT RNA was observed in tumor nodules by the systemic infection of the ribozyme-encoding virus. Such hTERT RNA knock-down *in vivo* induced changes in the global gene expression profile, including the suppression of specific genes associated with anti-apoptosis including *bcl2*, and genes for angiogenesis and metastasis. In addition, specific *trans*-splicing reaction with the targeted hTERT RNA took place in the tumors established as peritoneal carcinomatosis in mice by systemic deliv-

ery of the ribozyme. In conclusion, this study demonstrates that an hTERT-specific RNA replacement approach using *trans*-splicing ribozyme represents a potential modality to treat cancer.

Keywords: gene therapy; microarray analysis; RNA, catalytic; TERT protein, human; *trans*-splicing

Introduction

Telomerase is a multicomponent ribonucleoprotein located within the nucleus that synthesizes the repetitive nucleotide sequence forming the telomeres at the end of chromosomes (Morin, 1989). Telomerase activity appears to stabilize telomeres and allow the possibility of cellular immortality (Zhu *et al.*, 1999). Of note, telomerase activity is highly activated in 80-90% of malignant tissues and immortal cell lines (Kim *et al.*, 1994) and the activity is modulated mainly by the telomerase reverse transcriptase (TERT), the catalytic subunit of the telomerase. Therefore, TERT is a useful target for the development of anti-cancer agent.

The group I ribozyme from *Tetrahymena thermophila* was previously demonstrated to *trans*-splice an exon that is attached to its 3' end onto a separate 5' exon RNA, not only *in vitro* (Been and Cech, 1986) but also in *E. coli* (Sullenger and Cech, 1994) and mammalian cells (Jones *et al.*, 1996). We, as well as other groups, have shown that these group I-based *trans*-splicing ribozymes can revise mutant transcripts that are associated with several human genetic or malignant diseases (Lan *et al.*, 1998; Phylactou *et al.*, 1998; Watanabe and Sullenger, 2000; Rogers *et al.*, 2002; Shin *et al.*, 2004). Moreover, we demonstrated that *trans*-splicing ribozymes could selectively and specifically induce therapeutic gene activities in specific RNA-expressing cells through specific replacement of the target transcript (Ryu *et al.*, 2003). Accordingly, we developed human TERT (hTERT) RNA-replacing *trans*-splicing ribozyme that can stimulate the hTERT-dependent cytotoxicity in tumor cells (Kwon *et al.*, 2005). Furthermore, we recently showed that adenoviral vector harboring the ribozyme can either selectively mark tumor cells or selectively induce suicide gene activity in the tumors, thereby regressing the tumors with the

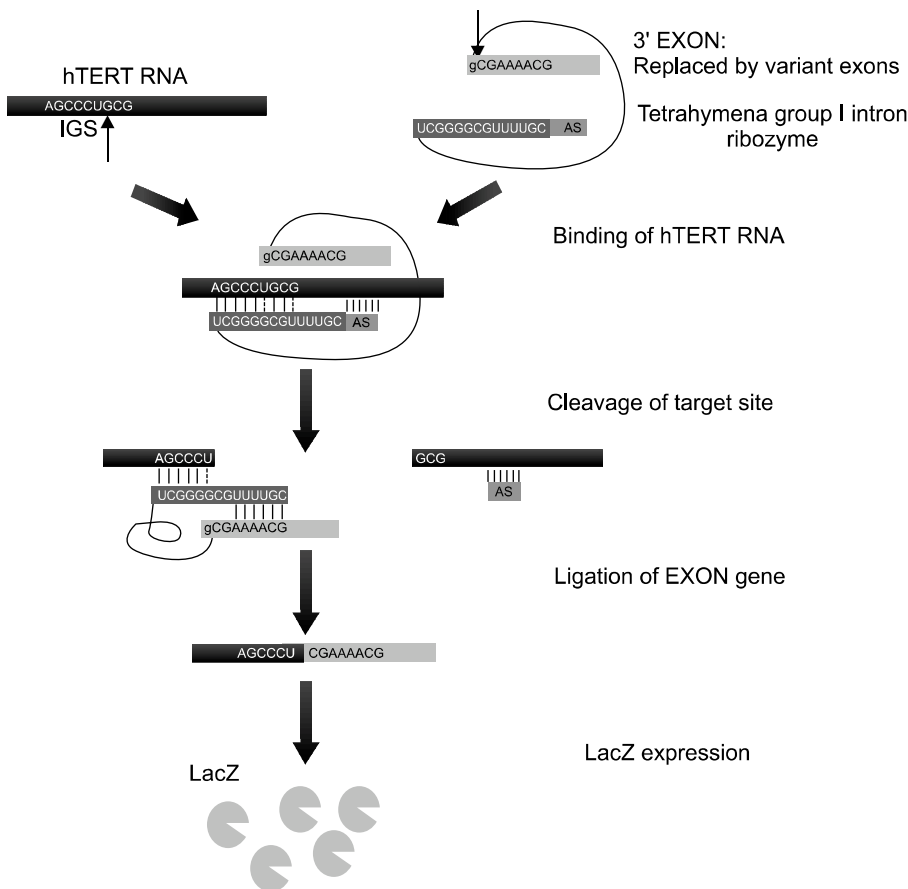


Figure 1. Scheme of ribozyme-mediated selective induction of new RNA coupled with reduction of target RNA by targeted *trans*-splicing of hTERT mRNA. A ribozyme can recognize hTERT RNA at accessible uridine residue by base pairing to the sequence through its internal guide sequence. The ribozyme then removes the sequence downstream of the target site and replaces it with a 3' exon that encodes a *lacZ* RNA sequence in this study.

prodrug treatment, in hTERT-expressing tumor xenografts (Hong *et al.*, 2007). These observations indicate that the *trans*-splicing ribozyme can be used as anti-cancer agents that reprogram cancer-specific transcripts to frustrate the cancerous cells.

The hTERT-specific *trans*-splicing ribozyme will be more effective as anti-cancer tool because it can induce therapeutic transgene activity selectively in the telomerase-positive cancer cells and can simultaneously reduce the hTERT RNA level in the cells (Figure 1). In this study, to evaluate the dual activity of the ribozyme and to analyze gene expression responses upon hTERT RNA reduction by the ribozyme *in vivo*, we observed any alterations of the gene expression profiles of tumor nodules in mice with intraperitoneal carcinomatosis after systemic delivery of the hTERT-targeting ribozyme.

Materials and Methods

Cell lines

The Hep3B cells (human hepatocellular carcinoma cell line) were purchased from the American Type

Culture Collection. The cells were maintained in Eagle minimal essential medium, supplemented with 10% heat-inactivated FBS (Join Bio-Innovation, Seoul, Korea), 50 U/ml penicillin G, and 50 µg/ml streptomycin (Sigma, St. Louis, MO) at 37°C in a humidified atmosphere of 5% CO₂.

Generation of recombinant adenoviral vectors

We constructed hTERT-specific *trans*-splicing ribozyme under the control of a phosphoenolpyruvate carboxykinase (PEPCK) promoter as previously described (Song and Lee, 2006). The expression of the specific ribozyme harboring diphtheria toxin A or HSVtk with the PEPCK promoter was shown to be the most effective and specific with regard to the retardation of the growth of hTERT⁺ liver cancer cells, as compared with other liver-specific promoters (Song and Lee, 2006). Recombinant adenovirus vector encoding the PEPCK promoter-derived hTERT-targeting ribozyme flanked by the cDNA for LacZ (β-galactosidase) as 3' exon (Figure 2A) was constructed using the *in vivo* homologous recombination technique in bacteria (BJ5183) with a type 5 adenoviral vector backbone

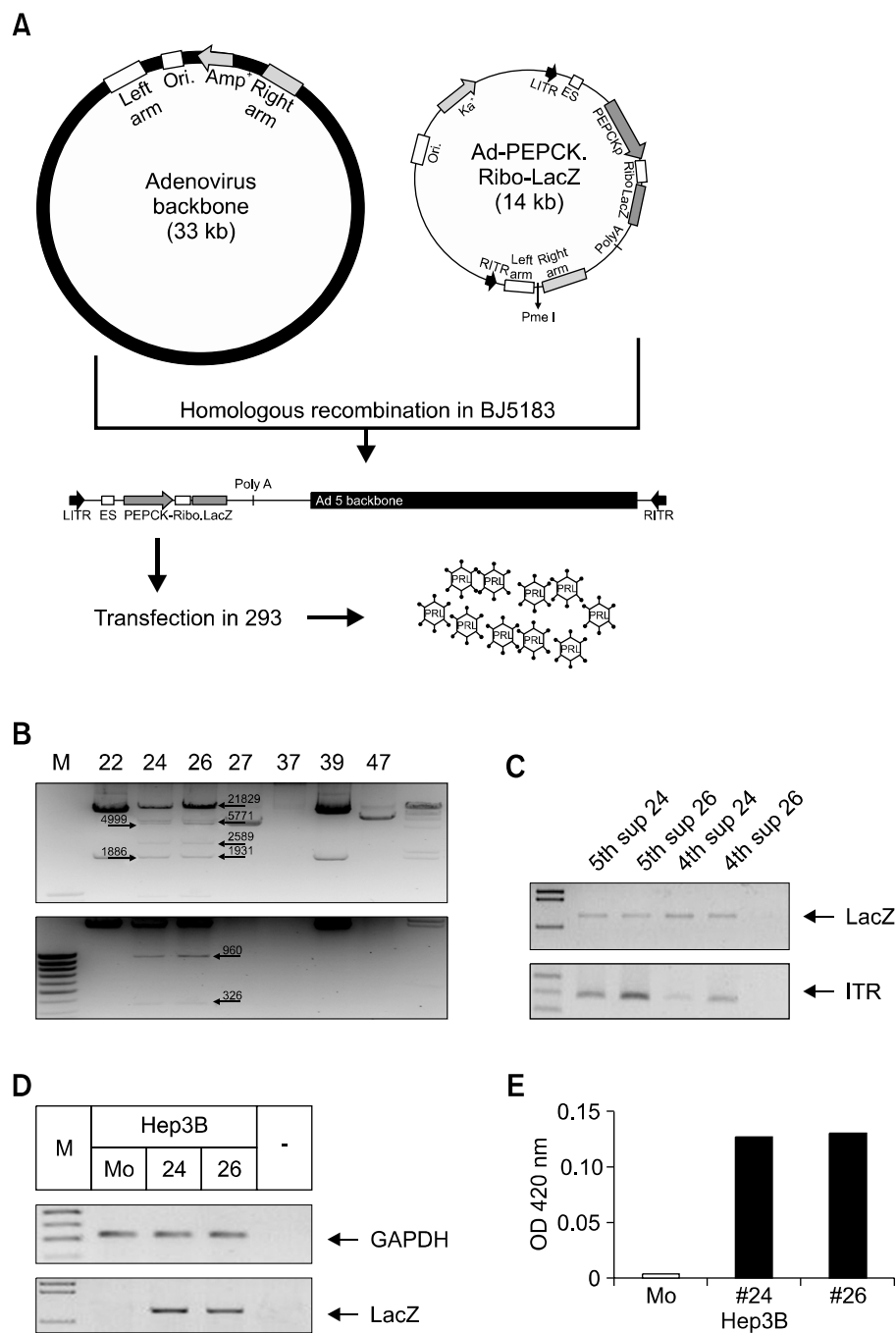


Figure 2. Characterization of recombinant adenovirus encoding the hTERT-specific ribozyme. (A) The PEPCK.Ribo-LacZ cassette was inserted into the E1 region of an Adenovirus type 5 backbone by homologous recombination in BJ5183. The resultant vector was transfected into 293 cells, and the recombinant viruses, Ad-PEPCK.Ribo-LacZ, were generated. (B) Each clone of recombinant viral vector generated by homologous recombination in BJ5183 cells was analyzed with *NotI*. Eight bands of restriction DNA fragments were then shown in the recombinant vectors as indicated with arrows. (C) PCR analysis of *lacZ* (280 bp) or ITR (210 bp) DNA from clone number 24 or 26 of the recombinant virus genomic DNA generated from 4th or 5th supernatant of the viral infected 293 cells. (D) RT-PCR analysis of GAPDH (210 bp) and *lacZ* (280 bp) RNA from Hep3B cells infected with clone number 24 or 26 of Ad-PEPCK.Ribo-LacZ. Mo represents mock-infected cells. (E) β -galactosidase activity of lysates from Hep3B cells infected with each clone of Ad-PEPCK.Ribo-LacZ.

in which the E1 and E3 region have been deleted (pAdenoVator Δ E1/E3 backbone E1/E3 deleted Ad5 genome, AdenoVectorTM, Qbiogene, Irvine, CA). Briefly, a *SpeI/BstBI* fragment containing the PEPCK promoter-Rib21AS-LacZ sequence was inserted into the pAdenoVator-CMV5-IRES-GFP shuttle vector. To construct recombinant virus vector, the shuttle plasmid was cleaved with *PmeI*. The linearized fragment was cotransformed into

BJ5183 cells with AdenoVectorTM. The recombinant vectors generated by homologous recombination in BJ5183 cells were isolated, analyzed with restriction enzymes, and linearized with *PacI*. The linearized vectors were then transfected into 293 cells and the produced recombinant adenoviruses were isolated by three rounds of plaque purification. Recombinant viruses were amplified using 293 cells, purified and concentrated by Vivapure[®]

AdenoPACK™ 100 (Sartorius AG, Edgewood, NY). Recombinant adenovirus was titered by determination of the TCID₅₀ (tissue culture infectious dose for 50% of the cells). We designated the recombinant adenovirus encoding for the ribozyme with *lacZ* under the control of the PEPCK promoter as Ad-PEPCK.Ribo-LacZ. An adenovirus with *lacZ* driven by the PEPCK promoter (Ad-PEPCK-LacZ) was employed as a control. Viral stocks were stored in 10% sucrose and kept at -80°C until use.

Molecular analysis of recombinant virus

Recombinant viral vector generated by homologous recombination in BJ5183 cells was confirmed by digestion with *NotI*. For the analysis of recombinant viral genomic DNA, viral supernatant generated in 293 cells were isolated, and the presence of *lacZ* and ITR gene was assessed using PCR. Viral supernatant from plaque isolation was infected into Hep3B. Total RNA was then isolated from the cell line and reverse transcribed with an oligo(dT) primer in the presence of 10 mM L-argininamide to confirm the promoter activity of the recombinant virus. The cDNAs were amplified with *lacZ* primer (5'-GGAATTCTGGTCGTTTTACAAC-GTCGTG-3' and 5'-GGGAAGCTTCGGATTGACC-GTAATGGGA-3'), or human GAPDH primer (5'-TGACATCAAGAAGGTGGTGA-3' and 5'-TGACAGACCCTGTTGCTG-3') as internal control. Infected cells were also used to measure β -galactosidase activity through incubation of cell extracts in 37°C for 2 h with *O*-nitrophenyl β -D-galactopyranoside (Sigma, St. Louis, MO) as a substrate.

Animals

Four- to 5-week-old male BALB/cAnNCrl nude mice (Orient Bio Inc., Seongnam, Korea) were used throughout this study. The animals were kept under specific pathogen-free (SPF) conditions and acclimated to laboratory conditions for at least 1 wk before use and maintained in Korean FDA animal facility in accordance with AAALAC International Animal Care policy (Accredited Unit-Korea Food and Drug Administration : Unit number-000996).

Intraperitoneal carcinomatosis animal model

For the peritoneal carcinomatosis model of Hep3B liver cancer cells, 2×10^7 Hep3B cells were intraperitoneally injected into BALB/c male nude mice. In the pilot investigation, the animals showed peritoneal carcinomatosis within 21 days, easily detectable with gross inspection and a binocular stereo-

microscope. To analyze specific transgene induction, we injected 1×10^9 pfu Ad-PEPCK-LacZ or Ad-PEPCK.Ribo-LacZ in PBS (total volume, 100 μ l) intraperitoneally three times with two day interval after the carcinomatosis establishment. Two days after the last virus injection, the established tumor tissues were removed.

RNA analysis

Following tumor dissection, total RNA was extracted using Tri-Reagent according to the manufacturer's protocol (Molecular Research Center Inc., Cincinnati, OH). After re-suspension in nuclease-free water, the RNA was quantified by UV spectroscopy (Bio-Rad, Hercules, CA), and qualified on a 2100 Bioanalyzer (Agilent, Palo Alto, CA).

To assess the reduction level of the hTERT RNA *in vivo* by the ribozyme, hTERT cDNA was amplified using real time PCR from 2 μ g total RNA of the hepatocarcinoma in mice two days after final adenovirus infection into intraperitoneal carcinomatosis mice model. Sequences of primers for the hTERT amplification are 5'-CGGAAGAGTGTCTG-GAGCAA-3' and 5'-GGATGAAGCGGAGTCTGGA-3'. All reagents except *Taq* polymerase (Takara, Otsu, Shiga, Japan) were obtained from the SYBR-Green core reagent kit (Molecular Probes, Eugene, OR). The protocol was followed as the manual of the PCR-kit [12.5 μ l SYBR Green Mix, 0.2 μ l cDNA, 1 μ l primer pair mix (5 pmol/ μ l each primer), and 11.3 μ l H₂O] (Oh *et al.*, 2006). The conditions for the PCR are at 95°C for 30 s, at 55°C for 40 s, and at 72°C for 1 min for 40 cycles. The relative kinetic method was applied using a standard curve constructed with 8-fold serial dilutions of hTERT gene obtained from the MCF7 breast cell line which was known to strongly express the hTERT gene (Villa *et al.*, 1998). The standard curve used for PCR is composed of 2 points (equivalent to 1 and 0.125 ng of hTERT PCR product). To control for the expression level of hTERT in the reaction mix, we used human GAPDH. The threshold levels obtained from the hTERT were adjusted to the threshold levels found in the GAPDH reaction to correct for minor variation in cDNA loading. For amplification, we used the Roter-Gene, a real time PCR machine (Corbett Life science, San Francisco, CA). To calculate relative quantification values, a threshold cycle (C_t), at which a statistically significant increase in fluorescence occurs, was derived from the resulting PCR profiles of each sample. C_t is a measure of the amount of template present in the starting reaction. To correct for different amounts of total cDNA in the starting reaction, C_t values for an endogenous control

(GAPDH) were subtracted from those of the corresponding hTERT level, resulting in ΔC_t . The relative quantification value of hTERT RNA level is expressed as $2^{-\Delta C_t}$ giving the relative difference of the ribozyme virus-treated sample compared to the control virus-infected sample.

Level of *bcl2* RNA and ribozyme RNA (LacZ) in the adenoviral injected tumor tissues were detected using RT-PCR of total RNA (Du *et al.*, 2006). Primers for the amplification are as follows: *bcl2*, 5'-CGGAATTCATTGTGGCTGCACTTGCT-3' and 5'-CCCAAGCTTCTGTTGCCCAACTGCAA-3'; LacZ, 5'-GGAATTCATGGTCGTTTTACAACGTCGTG-3' and 5'-GGGAAGCTTCGGATTGACCGTAA-TGGGA-3'. Production of *trans*-spliced molecules (TS) with targeted hTERT and the possibility of TS generation with *bcl2* RNA were assessed from the viral infected tumors. Total RNA was amplified with primers for TS with the hTERT RNA (5'-GGGGA-ATTCAGCGCTGCGTCCTGCT-3' and 5'-ATGGTC-GTTTTACAACGTCGTGAC-3') or with primers for TS with the *bcl2* RNA (5'-CGGAATTCATGTTGT-TGGCCGATCA-3' and 5'-ATGGTCGTTTTACAACGTCGTGAC-3').

Microarray analysis

We amplified and labeled total RNA from the hepatocarcinoma in mice infected with Ad-PEPCK-LacZ or Ad-PEPCK.Ribo-LacZ with Cy3-dCTP or Cy5-dCTP (Perkin Elmer, Boston, MA), respectively. RNA labeling was employed using the Agilent Low Input Linear Amplification kit according to the manufacturer's protocols. Each of Cy3 and Cy5 labeled cDNA (0.8 - 1 μ g) was combined and hybridized to 60-mer oligonucleotides microarray with sequences representing 41,194 human genes (Agilent, chip No. HWG251239143090). The slides were hybridized with GlassHyb buffer using the Lucidea SlidePro automated hybridization instrument (Amersham Biosciences, Piscataway, NJ) with the protocol for Agilent slide. The dried slides were then scanned with the GenePix 4000B Microarray Scanner, and the initial images captured by the GenePix Pro 4.1 software (Axon Instruments, Union City, CA). The data were analyzed using Acuity software Version 3.1 (Axon Instruments).

Results

Construction of recombinant adenovirus

Expression vector for the hTERT-targeting ribozyme was constructed through the incorporation of a PEPCK.Ribo-LacZ sequence into a type 5 ade-

noviral vector backbone (Figure 2A). The resulting plasmid is then linearized and co-transformed into *E.coli* strain BJ5183 with adenovirus backbone DNA in which the E1 and E3 region have been deleted. Recombinant viral vectors resulting from homologous recombination are selected with kanamycin and screened by restriction enzyme analysis. A restriction digest with *NotI* gives a restriction pattern as shown in Figure 2B (8 bands with size of 21829, 5571, 4999, 2589, 1931, 1886, 960 and 326 bp). The recombinants were digested with *PacI* and transfected into 293 cells, where the E1 functions can be complemented, by calcium phosphate transfection method to allow production of recombinant adenoviral DNA and packaging into virions. Viral plaques generated in 293 cells were isolated and expanded. After 5 rounds of plaque purification, the expression cassette in the adenoviral vectors was confirmed by PCR of viral genomic DNA and *lacZ* gene using specific primer (Figure 2C).

Recombinant viruses were amplified using 293 cells, purified and concentrated, and β -galactosidase assay were performed to examine the expression of the *lacZ* 48 h after infection with either clone number 24 or 26 of recombinant virus into hTERT⁺ Hep3B cells. As shown in Figure 2D and E, expression of *lacZ* was detected not only at RNA level but also at protein level in the adenoviral vector-infected Hep3B cells. In contrast, no β -galactosidase was observed in hTERT⁻ SK-LU-1 cells infected with the virus (data not shown). These results demonstrate that the recombinant viral vectors successfully and selectively induce the expression of transgene, *lacZ*, in liver cancer cells.

Microarray analysis of TERT-dependent gene expression

To determine which transcripts are affected *in vivo* by the hTERT-targeting *trans*-splicing ribozyme and to assess the specificity of the ribozyme, we first established animal model with peritoneal carcinomatosis by intraperitoneal transplantation of Hep3B cells into nude mice. Then, we systemically infected adenoviral vector encoding the ribozyme into the mice, and studied the gene expression profile using oligonucleotide microarray experiments in the tumor nodules established in the mice. Changes in the mRNA levels of tumor nodules were analyzed by comparing tumors injected with virus encoding the hTERT-targeting ribozyme (Ad-PEPCK.Ribo-LacZ, PRL) with those that were infected with control virus (Ad-PEPCK-LacZ, PL).

Table 1. Gene expression profile in HCC following injection of peritoneal carcinomatosis mice with Ad-PEPCK.Ribo-LacZ.

Probe ID	Symbol	Name	Synonyms	Fold change*
Apoptosis				
<i>Anti-apoptosis</i>				
A_23_P42935	BRAF	V-raf murine sarcoma viral oncogene homolog B1	BRAF1, B-raf 1, B-Raf proto-oncogene serine/threonine-protein kinase, MGC126806, MGC138284, p94, RAFB1, v-Raf murine sarcoma viral oncogene homolog B1	2.169 ↓
A_24_P192485	TNFRSF11B	Tumor necrosis factor receptor superfamily, member 11b (osteoprotegerin)	MGC29565, OCIF, OPG, Osteoclastogenesis inhibitory factor, Osteoprotegerin, TR1, Tumor necrosis factor receptor superfamily member 11B precursor	2.392 ↓
A_24_P917766	BIRC6	Baculoviral IAP repeat-containing 6 (apollon)	APOLLON, Baculoviral IAP repeat-containing protein 6, BRUCE, FLJ13726, FLJ13786, KIAA1289, Ubiquitin-conjugating BIR-domain enzyme apollon	5.650 ↓
A_23_P115444	TNFSF18	Tumor necrosis factor (ligand) superfamily, member 18	Activation-inducible TNF-related ligand, AITRL, GITRL, Glucocorticoid-induced TNF-related ligand, hGITRL, MGC138237, TL6, Tumor necrosis factor ligand superfamily member 18, UNQ149/PRO175	6.410 ↓
A_24_P512775	BCL2	B-cell CLL/lymphoma 2	Apoptosis regulator Bcl-2	8.621 ↓
<i>Induction of apoptosis</i>				
A_23_P218646	TNFRSF6B	Tumor necrosis factor receptor superfamily, member 6b, decoy	DcR3, DCR3, Decoy receptor 3, Decoy receptor for Fas ligand, DJ583P15.1.1, M68, TR6, Tumor necrosis factor receptor superfamily member 6B precursor, UNQ186/PRO212	2.596 ↑
A_23_P138635	BNIP3	BCL2/adenovirus E1B 19 kDa interacting protein 3	BCL2/adenovirus E1B 19-kDa protein-interacting protein 3, Nip3, NIP3	2.469 ↑
A_23_P111343	BCLAF1	BCL2-associated transcription factor 1	Bcl-2-associated transcription factor 1, bK211L9.1, Btf, BTF, KIAA0164	2.162 ↑
A_23_P346311	BAX	BCL2-associated X protein	Apoptosis regulator BAX, cytoplasmic isoform beta, Apoptosis regulator BAX, membrane isoform alpha, BAX protein, cytoplasmic isoform delta, BAX protein, cytoplasmic isoform gamma	2.083 ↑
<i>Induction of apoptosis resulting from DNA damage response signal transduction</i>				
A_23_P60180	ABL1	V-abl Abelson murine leukemia viral oncogene homolog 1	Abelson murine leukemia viral oncogene homolog 1, ABL, c-ABL, JTK7, p150, Proto-oncogene tyrosine-protein kinase ABL1, v-abl	2.193 ↑
<i>Caspase</i>				
A_24_P269398	CASP2	Caspase 2, apoptosis-related cysteine peptidase	CASP-2, Caspase-2 precursor, ICH1, ICH-1L, ICH-1L/1S, ICH-1 protease, NEDD2	1.996 ↑
A_23_P35906	CASP4	Caspase 4, apoptosis-related cysteine peptidase	CASP-4, Caspase-4 precursor, ICE(rel)II, ICE(rel)-II, ICEREL-II, ICH2, ICH-2, ICH-2 protease, Mih1/TX, TX, TX protease	1.733 ↑
A_24_P111342	CASP9	Caspase 9, apoptosis-related cysteine peptidase	APAF3, APAF-3, Apoptotic protease-activating factor 3, Apoptotic protease Mch-6, CASP-9, CASPASE-9c, Caspase-9 precursor, ICE-LAP6, ICE-like apoptotic protease 6, MCH6	1.705 ↑

*A subset of genes involved in apoptosis, angiogenesis and tumor metastasis, expression of which was increased (↑) or decreased (↓) more than 2-fold by treatment of Ad-PEPCK.Ribo-LacZ when compared with inoculation of the control adenovirus (Ad-PEPCK-LacZ), are shown. In accordance with the real-time PCR data in Figure 3D, level of hTERT mRNA was decreased 6.85 fold by the specific ribozyme.

Only two days after systemic delivery of the PRL into the intraperitoneal carcinomatosis mice, we observed a ≥ 2 -fold change of RNA level in 1,189 genes including hTERT gene out of surveyed 41,194 human genes in the established human hepatocellular carcinoma (HCC). Some of genes whose expression was changed by PRL are in-

involved in apoptosis or tumorigenesis pathway, as shown in the microarray data with siRNA treatment against hTERT or RNA subunit of telomerase, hTER (Li *et al.*, 2005; Shammam *et al.*, 2005) (Table 1). Expression of genes involved in the process of anti-apoptosis was efficiently down-regulated by PRL. Specific genes that have been

Table 1. Continued.

Probe ID	Symbol	Name	Synonyms	Fold change*
Angiogenesis				
A_24_P167012	TNFSF15	Tumor necrosis factor (ligand) superfamily, member 15	MGC129934, MGC129935, TL1, TL1A, TNF ligand-related molecule 1, Tumor necrosis factor ligand superfamily member 15, Vascular endothelial cell growth inhibitor, VEGI, VEGI192A	4.032 ↓
A_24_P388810	APC	Adenomatosis polyposis coli	Adenomatous polyposis coli protein, DP2, DP2.5, DP3, FAP, FPC, GS, Protein APC	4.902 ↓
A_24_P402438	TGFB2	Transforming growth factor, beta 2	BSC-1 cell growth inhibitor, Cetermin, Glioblastoma-derived T-cell suppressor factor, G-TSF, MGC116892, Polyergin, TGF-beta2, TGF-beta-2, Transforming growth factor beta-2 precursor	5.714 ↓
A_32_P100379	PDGFRA	Platelet-derived growth factor receptor, alpha polypeptide	Alpha platelet-derived growth factor receptor precursor, CD140a, CD140A, CD140a antigen, MGC74795, PDGFR2, PDGF-R-alpha	6.250 ↓
A_23_P381992	ITGAV	Integrin, alpha V (vitronectin receptor, alpha polypeptide, antigen CD51)	CD51, CD51 antigen, Integrin alpha-V precursor, MSK8, Vitronectin receptor alpha subunit, VNRA	6.452 ↓
A_23_P428139	EFNB2	Ephrin-B2	EPH-related receptor tyrosine kinase ligand 5, Ephrin-B2 precursor, EPLG5, HTKL, Htk-L, HTK-L, HTK ligand, LERK5, LERK-5, MGC126226, MGC126227, MGC126228	6.623 ↓
Tumor metastasis				
A_23_P208126	SERPINB5	Serpin peptidase inhibitor, clade B (ovalbumin), member 5	Maspin, PI5, Protease inhibitor 5, Serpin B5 precursor	2.155 ↓
A_23_P9513	MTA1	Metastasis associated 1	Metastasis-associated protein MTA1	2.278 ↓
A_23_P94800	S100A4	S100 calcium binding protein A4 (calcium protein, calvasculin, metastasin, murine placental homolog)	18A2, 42A, Calvasculin, CAPL, Metastasin, MTS1, Mts1 protein, P9KA, PEL98, Placental calcium-binding protein, Protein S100-A4, S100 calcium-binding protein A4	2.392 ↓
A_24_P33140	TIMP3	TIMP metalloproteinase inhibitor 3 (Sorsby fundus dystrophy, pseudoinflammatory)	HSMRK222, K222, K222TA2, Metalloproteinase inhibitor 3 precursor, MIG-5 protein, SFD, TIMP-3, Tissue inhibitor of metalloproteinases-3	2.994 ↓
A_24_P929003	ITGB3	Integrin, beta 3 (platelet glycoprotein IIIa, antigen CD61)	CD61, CD61 antigen, GP3A, GPIIIa, Integrin beta-3 precursor, Platelet membrane glycoprotein IIIa	4.237 ↓
A_24_P388810	APC	Adenomatosis polyposis coli	Adenomatous polyposis coli protein, DP2, DP2.5, DP3, FAP, FPC, GS, Protein APC	4.902 ↓
A_23_P71073	TWIST1	Twist homolog 1 (acrocephalosyndactyly 3; Saethre-Chatzen syndrome) (Drosophila)	ACS3, BPES2, BPES3, H-twist, SCS, TWIST, Twist-related protein 1	7.813 ↓

found to play important roles in angiogenesis or metastasis were also down-regulated. Some of genes which were up-regulated were participated in apoptosis induction process. In contrast, no significant alteration in the expression level of genes involved in immune response including cytokines, interferons, or interferon-stimulated genes was observed by PRL injection, suggesting that ribozyme expression via PRL treatment of mice did not induce dsRNA-mediated nonspecific interferon response in the established HCC.

Effects on hTERT RNA level by Ad-PEPCK.Ribo-LacZ

To verify the results obtained from the microarray experiments, we assessed RNA level of hTERT genes by real time quantitative PCR using the SYBR Green method (Figure 3A). Expression level

of the housekeeping gene, GAPDH, showed only minor difference between PL- or PRL-infected tumor groups and served as both a control for RT-PCR performance and a reference for relative quantification (Figure 3B). The analytical sensitivity of the real-time RT-PCR was determined with a series of dilutions of RT-PCR product (1 and 0.125 ng) of hTERT RNA. Amplification of the hTERT RNA transcripts at different concentrations showed linearity, and R^2 was 0.99 (Figure 3C). The threshold cycle number (Ct) of PCR of the hTERT RNA in tumors infected with PRL (Ct = 15.1) was higher than that with PL (Ct = 12.8) (Figure D). These results strongly suggest that the level of hTERT RNA was more than 4 fold reduced in tumors by the adenovirus encoding the hTERT-specific ribozyme, compared with the control virus.

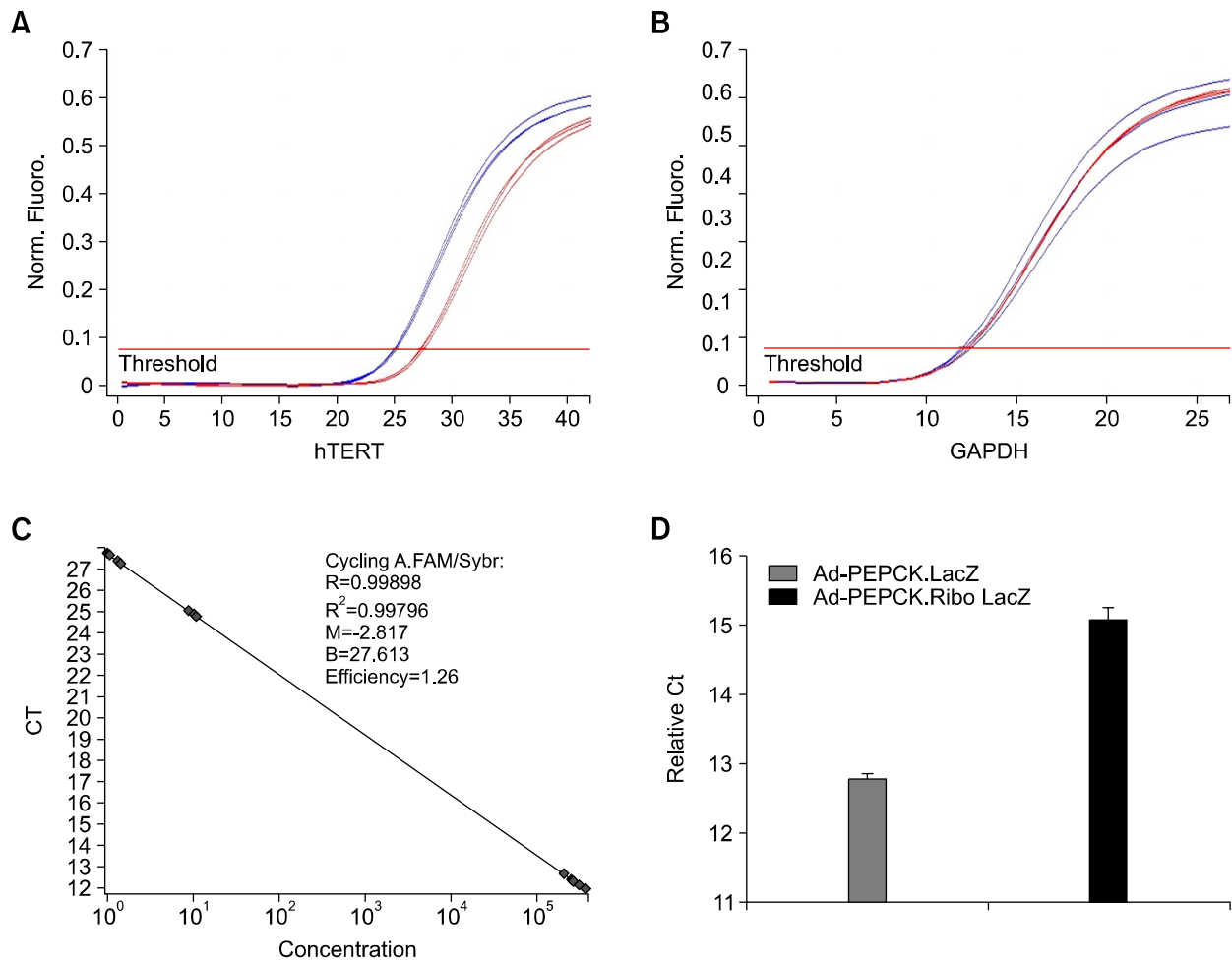


Figure 3. Real-time PCR analysis of hTERT (A) and GAPDH (B) mRNA amounts in tumor nodules infected by Ad-PEPCK-LacZ (blue line) or Ad-PEPCK.Ribo-LacZ (red line); (C) Linear plot of Ct in each sample was plotted against concentration of standard hTERT cDNA, $R^2 = 0.99$ (D) The threshold cycle (C_t) of hTERT RNA in each viral infected tumor was normalized against C_t of GAPDH RNA in the corresponding sample.

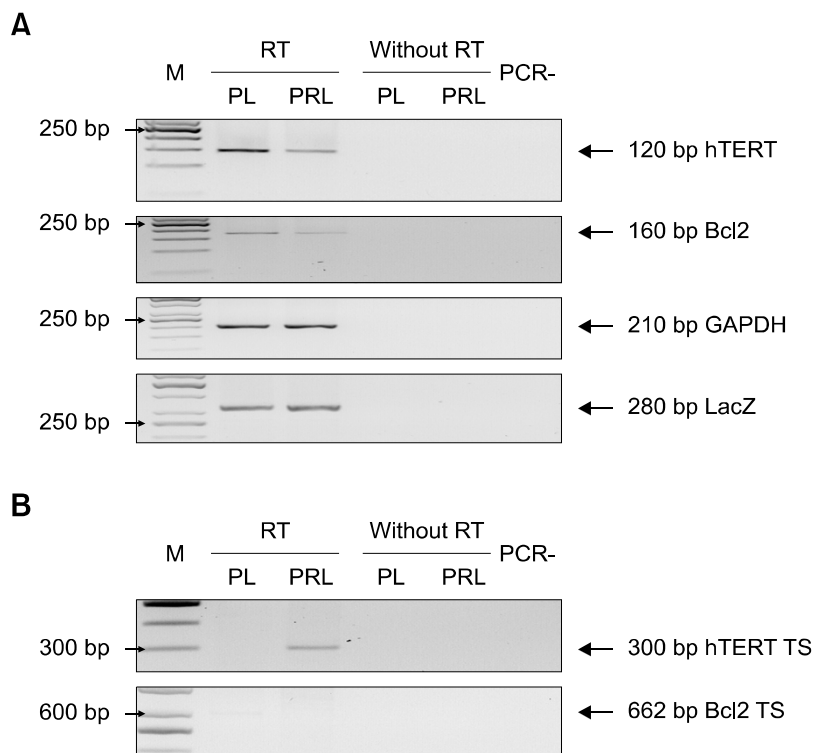


Figure 4. RNA expression patterns in tumor tissues of mice with peritoneal carcinomatosis after injection of Ad-PEPCK-LacZ (PL) or Ad-PEPCK.Ribo-LacZ (PRL). (A) Level of hTERT, *bcl2*, and ribozyme RNA (LacZ) were detected using RT-PCR of total RNA in the adenovirally injected tumor tissues. As an internal control, the 210 bp amplified RNA product of human GAPDH is presented for each sample. (B) Production of *trans*-spliced molecules (TS) with targeted hTERT and the possibility of TS generation with *bcl2* RNA were assessed from the viral infected tumors.

Analysis of gene expression affected by Ad-PEPCK.Ribo-LacZ

Using RT-PCR analysis, we confirmed PRL-mediated downregulation of the *bcl2* gene expression, which was found to decrease more than 8 fold from the microarray analysis (Figure 4A). In contrast with generation of *trans*-splicing product with the targeted hTERT RNA by PRL, no *trans*-splicing was created with *bcl2* RNA, indicating that at least the reduction of *bcl2* gene expression was not due to nonspecific *trans*-splicing reaction with the hTERT-targeting ribozyme (Figure 4B). Moreover, RACE RT-PCR and sequencing analysis revealed that all of the *trans*-splicing products generated in HCC of the PRL-injected mice were from reactions only with the targeted hTERT RNA, implying target specificity of the *trans*-splicing ribozyme *in vivo* (data not shown). Collectively with the microarray analysis, these results indicated that PEPCK promoter-driven *trans*-splicing ribozyme specifically replaced the hTERT RNA and efficiently reduced RNA level of the target *in vivo*, resulting in alteration in the global gene expression pattern indicative of novel response pathway such as induction of apoptosis and suppression of angiogenesis or metastasis.

Discussion

The aim of this study was to validate *in vivo* function of hTERT-targeting *trans*-splicing ribozymes with molecular analysis of affected gene expression. The hTERT-specific *trans*-splicing ribozyme will be more advantageous than other anti-cancer agents because the ribozyme could selectively induce targeted expression of the therapeutic gene product in hTERT⁺ cancer cells and simultaneously decrease in the level of target hTERT transcript, hence reducing endogenous telomerase activity. To broadly screen for molecular effects by the hTERT-specific ribozyme, we performed oligonucleotide microarray analysis of peritoneal carcinomatosis infected with the ribozyme-encoding adenovirus using the Whole Human Genome Oligo Microarray Kit from agilent, which represent all known genes and transcripts in the human genome. As expected, the level of hTERT RNA in tumors was significantly reduced by systemic delivery of PRL encoding the specific ribozyme. Moreover, approximately 3% of the whole human genes were changed in their expression level in tumors infected with PRL, compared with tumors with PL. No significant difference in the β -galactosidase activity was observed between tumors infected with PL and PRL (data not shown). Thus, this alteration might not be due to LacZ expression

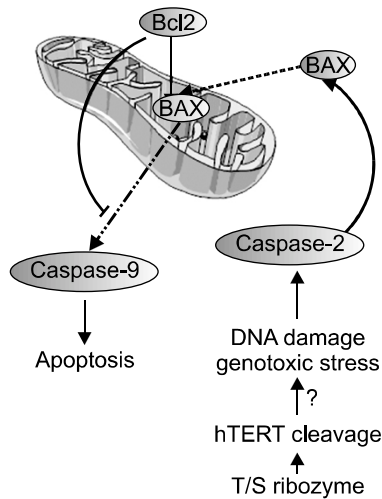


Figure 5. Scheme of potential pathway to induce mitochondrial apoptosis through hTERT reduction mediated by *trans*-splicing (T/S) ribozyme.

induced by the ribozyme but due to the inhibition of the hTERT RNA level.

Gross changes were observed two days after the adenovirus infection in the expressional levels of various genes involved in apoptosis and tumorigenesis, which may in part explain other findings that human cancer cells have a rapid and defined growth inhibitory response to telomerase depletion, even without telomere shortening (Folini *et al.*, 2003; Li *et al.*, 2004, 2005). It is remarkable that the vast majority of apoptosis regulators which were down-regulated in ribozyme-expressing tumor nodules are proapoptotic genes. At this point, it is difficult to draw conclusions how hTERT may interact within the apoptotic cascade. However, the result of this experiment indicated the kinds of dysregulated genes, and therefore, could further guide our research direction regarding TERT function. The apoptosis regulating function of hTERT will be complicated, as suggested by a recent study describing the role of telomerase on apoptosis through modulation of Bcl2 expression (Del Buffalo *et al.*, 2005). In this study, we observed *in vivo* molecular associations between the level of hTERT mRNA and *bcl2* transcript, which resulted from systemic delivery of the hTERT-specific *trans*-splicing ribozyme (Figure 5), in agreement with the observation by Del Buffalo *et al.* (2005), who showed that the inhibition of telomerase expression induced mitochondrial apoptosis by targeted intervention in Bcl2 expression and function. hTERT overexpression was also shown to interfere at an early stage of cell death pathway involved in mitochondrial alterations (Massard *et al.*, 2006). Moreover, telomerase was recently demonstrated

to not only stabilize telomeres but also activate the expression of proliferation enhanced genes (Smith *et al.*, 2003). Furthermore, nuclear-targeted hTERT showed enhanced antiapoptotic activity by inhibition of nuclear export of endogenous hTERT in human embryonic kidney cells (Haendeler *et al.*, 2003). These results together with our gene expression profile data suggest that hTERT may directly or indirectly modulates the expression of genes implicated in intrinsic apoptosis pathway controlled by *bcl2*.

In conclusion, this study points to *in vivo* function of the hTERT-specific *trans*-splicing ribozyme. The ribozyme efficiently reduced the hTERT RNA level, which in turn reduced gene expression involved in anti-apoptosis, angiogenesis and tumor metastasis. The observation of the relation of apoptosis, angiogenesis and tumor metastasis with the activity and/or expression level of telomerase will be positively influential to design telomerase-targeting agent as anti-cancer modality because the level of these pathways noticeably affects tumor growth. Moreover, at the same time with global change of gene expression, the hTERT-specific ribozyme induced target-dependent generation of *trans*-splicing RNA product *in vivo*. Therefore, present study proves potential usefulness of the RNA replacement strategy with hTERT-specific *trans*-splicing ribozyme as therapeutic approach to cancer.

Acknowledgements

This work was supported by the Korea Science and Engineering Foundation (M1053400004-06N3400-00410). M.S. Song is a recipient of Brain Korea 21 fellowship.

References

- Been MD, Cech TR. One binding site determines sequence specificity of Tetrahymena pre-rRNA self-splicing, trans-splicing, and RNA enzyme activity. *Cell* 1986;47:207-16
- Del Buffalo D, Rizzo A, Trisciuglio D, Cardinali G, Torrisi MR, Zangemeister-Wittke U, Zupi G, Biroccio A. Involvement of hTERT in apoptosis induced by interference with Bcl-2 expression and function. *Cell Death Differ* 2005;12:1429-38
- Du ZX, Zhang HY, Gao DX, Wang HQ, Li YJ, Liu GL. Antisurvivin oligonucleotides inhibit growth and induce apoptosis in human medullary thyroid carcinoma cells. *Exp Mol Med* 2006;38:230-40
- Folini M, Berg K, Millo E, Villa R, Prasmickaite L, Daidone MG, Benatti U, Zaffaroni N. Photochemical internalization of a peptide nucleic acid targeting the catalytic subunit of human telomerase. *Cancer Res* 2003;63:3490-4
- Haendeler J, Hoffmann J, Brandes RP, Zeiher AM, Dimmeler

S. Hydrogen peroxide triggers nuclear export of telomerase reverse transcriptase via Src kinase family-dependent phosphorylation of tyrosine 707. *Mol Cell Biol* 2003;23:4598-610

Hong SH, Jeong JS, Lee YJ, Jung HI, Cho KS, Kim CM, Kwon BS, Sullenger BA, Lee SW, Kim IH. *In vivo* reprogramming of hTERT by trans-splicing ribozyme to target tumor cells. *Mol Ther* 2007; Epub ahead of print

Jones JT, Lee SW, Sullenger BA. Tagging ribozyme reaction sites to follow trans-splicing in mammalian cells. *Nat Med* 1996;2:643-8

Kim NW, Piatyszek MA, Prowse KR, Harley CB, West MD, Ho PL, Coviello GM, Wright WE, Weinrich SL, Shay JW. Specific association of human telomerase activity with immortal cells and cancer. *Science* 1994;266:2011-5

Kwon BS, Jung HS, Song MS, Cho KS, Kim SC, Kimm K, Jeong JS, Kim IH, Lee SW. Specific regression of human cancer cells by ribozyme-mediated targeted replacement of tumor-specific transcript. *Mol Ther* 2005;12:824-34

Lan N, Howrey RP, Lee SW, Smith CA, Sullenger BA. Ribozyme-mediated repair of sickle β -globin mRNAs in erythrocyte precursors. *Science* 1998;280:1593-6

Li S, Rosenberg JE, Donjacour AA, Botchkina IL, Hom YK, Cunha GR, Blackburn EH. Rapid inhibition of cancer cell growth induced by lentiviral delivery and expression of mutant-template telomerase RNA and anti-telomerase short-interfering RNA. *Cancer Res* 2004;64:4833-40

Li S, Crothers J, Haqq CM, Blackburn EH. Cellular and gene expression responses involved in the rapid growth inhibition of human cancer cells by RNA interference-mediated depletion of telomerase RNA. *J Biol Chem* 2005;280:23709-17

Massard C, Zermati Y, Pauleau AL, Larochette N, Métévier D, Sabatier L, Kroemer G, Soria JC. hTERT: a novel endogenous inhibitor of the mitochondrial cell death pathway. *Oncogene* 2006;25:4505-14

Morin GB. The human telomere terminal transferase enzyme is a ribonucleoprotein that synthesizes TTAGGG repeats. *Cell* 1989;59:521-9

Oh DY, Jung KH, Yang BH, Lee JS, Choi IG, Chai YG. Naltrexone influences protein kinase C ϵ and integrin α 7

activity in SH-SY5Y neuroblastoma cells. *Exp Mol Med* 2006;38:100-6

Phylactou LA, Darrah C, Wood MJ. Ribozyme-mediated trans-splicing of a trinucleotide repeat. *Nat Genet* 1998;18:378-81

Rogers CS, Vanoye CG, Sullenger BA, George AL Jr. Functional repair of a mutant chloride channel using a trans-splicing ribozyme. *J Clin Invest* 2002;110:1783-9

Ryu KJ, Kim JH, Lee SW. Ribozyme-mediated selective induction of new gene activity in hepatitis C virus internal ribosome entry site-expressing cells by targeted trans-splicing. *Mol Ther* 2003;7:386-95

Shammas M, Koley H, Batche R, Bertheau RC, Protopopov A, Munshi NC, Goyal RK. Telomerase inhibition by siRNA causes senescence and apoptosis in Barrett's adenocarcinomas cells: mechanism and therapeutic potential. *Mol Cancer* 2005;4:24

Shin KS, Sullenger BA, Lee SW. Ribozyme-mediated induction of apoptosis in human cancer cells by targeted repair of mutant p53 RNA. *Mol Ther* 2004;10:365-72

Smith LL, Collier HA, Roberts JM. Telomerase modulates expression of growth-controlling genes and enhances cell proliferation. *Nat Cell Biol* 2003;5:474-9

Song MS, Lee SW. Cancer-selective induction of cytotoxicity by tissue-specific expression of targeted trans-splicing ribozyme. *FEBS Lett* 2006;580:5033-43

Sullenger BA, Cech TR. Ribozyme-mediated repair of defective mRNA by targeted, trans-splicing. *Nature* 1994;371:619-22

Villa R, Zaffaroni N, Folini M, Martelli G, De Palo G, Daidone MG, Silvestrini R. Telomerase activity in benign and malignant breast lesions: a pilot prospective study on fine-needle aspirates. *J Natl Cancer Inst* 1998;90:537-9

Watanabe T, Sullenger BA. RNA repair: a novel approach to gene therapy. *Adv Drug Deliv Rev* 2000;44:109-18

Zhu J, Wang H, Bishop JM, Blackburn EH. Telomerase extends the lifespan of virus-transformed human cells without net telomere lengthening. *Proc Natl Acad Sci USA* 1999;96:3723-8